Myocardial Stiffness, Cardiac Remodeling, and Diastolic Dysfunction in Calcification-Prone Fetuin-A–Deficient Mice

Marc W. Merx,* Cora Schäfer,† Ralf Westenfeld,‡ Vincent Brandenburg,†‡ Sylvia Hidajat,* Christian Weber,*§ Markus Ketteler,‡ and Willi Jahnen-Dechent†

Medical Clinic I, †IZKF BIOMAT, ‡Medical Clinic II, and §Department of Cardiovascular Molecular Biology, RWTH University Hospital, Aachen, Germany

Accelerated atherosclerosis in dialysis patients is characterized by severe vascular calcification, and the magnitude of vascular calcification is associated with increased cardiovascular mortality. Calcification-dependent arterial stiffness is considered to be a major determinant of cardiac failure in uremia. Fetuin-A/α_2-Heremans-Schmid glycoprotein is an abundant serum protein with powerful calcification inhibitory properties. Fetuin-A deficiency was recently linked to cardiovascular mortality in dialysis patients. Fetuin-A knockout (fetuin-KO) mice spontaneously develop widespread soft tissue calcification, including significant myocardial calcification, whereas larger arteries are spared. Therefore, this investigation offers the unique opportunity to study the functional role of isolated myocardial calcification independent of arterial stiffness by assessing the hemodynamics of fetuin-KO mice. Cardiac output in fetuin-KO mice was lower than in wild-type mice (fetuin-KO 1.81 ± 0.18 *versus* WT 2.45 ± 0.29 ml/min per g; $P < 0.005$), and fetuin-KO mice were refractory to dobutamine stimulation. Left ventricular relaxation was significantly impaired in fetuin-KO hearts with the relaxation index reduced by 23% ($P < 0.005$). After ischemia, fetuin-KO hearts displayed a continuous decline in left ventricular developed pressure after the initial phase of reperfusion, resulting in 77 ± 15% of preischemic left ventricular developed pressure ($P < 0.05$ *versus* wild-type). In fetuin-KO mice, dystrophic cardiac calcification, with myocardial calcium contents increased 60-fold, was associated with profound induction of profibrotic TGF-β and downstream collagen and fibronectin mRNA synthesis. In conclusion, independent of arterial stiffness, calcification-associated "myocardial stiffness" characterized by cardiac fibrosis, diastolic dysfunction, impaired tolerance to ischemia, and catecholamine resistance thus may constitute an underestimated cardiovascular risk factor that contributes to cardiac failure in calcification-prone states.

J Am Soc Nephrol 16: 3357–3364, 2005. doi: 10.1681/ASN.2005040365

Fetuin-A/α_2-Heremans-Schmid glycoprotein (Ahsg) is a liver-derived negative acute-phase protein present in all extracellular fluids (1). Owing to its high affinity for calcium phosphates, fetuin-A accumulates in the mineralized bone matrix, in atherosclerotic plaques, and in pathologically mineralized tissues (2,3). Mineral binding is a salient feature of fetuin-A biology, but it also binds to multiple ligands, including the fibrogenic growth factor TGF-β, thus acting as a soluble receptor-like antagonist of TGF-β actions (4). Chemically, fetuin-A acts as an inhibitor of spontaneous calcium phosphate precipitation by forming soluble colloidal calciprotein particles that contain fetuin, calcium, and phosphate (5,6). On the cellular level, fetuin-A accumulates in mineralization-competent matrix vesicles associated with vascular smooth muscle cells, thus attenuating apoptosis and dystrophic calcification (7). *In vivo*, fetuin-A deficiency in DBA/2 mice is associated with spontaneous widespread dystrophic soft tissue calcification, especially in the kidney, lung, and heart but sparing the aorta (8). A cross-sectional study identified low fetuin-A serum concentrations as a predictor of cardiovascular mortality in hemodialysis patients, a population of patients who are prone to develop severe extraosseous calcifications and experience a highly increased cardiovascular mortality (9). Combined, these data demonstrate that fetuin-A is a major inhibitor of calcification acting systemically in blood and extracellular fluids.

Cardiovascular tissues seem to be especially prone to dystrophic calcification. In fact, age-related dystrophic calcification is frequently encountered in human coronary artery disease and various other cardiac disease conditions. It has even been postulated that dystrophic calcification might contribute to cardiac dysfunction with at least the same prevalence as ischemic heart disease (10). In dialysis patients, the magnitude of cardiovascular calcification is especially high, affecting atherosclerotic plaques, arterial media, cardiac valves, and the myocardium, respectively (11–15). The severity of medial calcification is associated with arterial stiffness and increased pulse wave velocity (16). This in turn increases afterload and end-systolic left ventricular pressures during every heart beat by way of decreased aortic compliance and premature repercussion of the systolic pulse wave. Collectively, these phenomena are thought to be pathophysiologically involved in the development of left

Received April 6, 2005. Accepted August 13, 2005.

Published online ahead of print. Publication date available at www.jasn.org.

M.W.M. and C.S. contributed equally to this work.

Address correspondence to: Dr. Marc W. Merx, Medizinische Klinik I, Universitätsklinikum RWTH Aachen, Pauwelsstrasse 30, Aachen, Germany D-52057. Phone: +49-241-8089300; Fax: +49-241-8082545; E-mail: mmerx@ukaachen.de

ISSN: 1046-6673/1611-3357

ventricular dysfunction and congestive heart failure in the dialysis population. There are, however, no data available on the potential direct impact of myocardial calcification on left ventricular dysfunction or cardiovascular outcome.

Despite this high prevalence and clinical significance of cardiovascular dystrophic calcification, the limited availability of experimental data are largely due to a lack of adequate animal models. Fetuin-KO mice experience massive myocardial calcification and die prematurely, but most of these animals survive to adulthood and therefore can be subjected to functional hemodynamic studies. Here, we present a study of cardiac calcification, remodeling, and function in these animals to gain mechanistic insight into heart failure secondary to dystrophic myocardial calcification and independent of the major confounding factor, arterial calcification and consecutive arterial stiffness.

Materials and Methods

Animals

All animal experiments in this study were performed in compliance with the German Animal Protection Law after approval of procedures by state animal protection boards. Mice were kept in a barrier facility under a 12-h day/night cycle with *ad libitum* access to water and standard chow (Altromin 1324; Altromin GmbH, Lage, Germany). All *in vivo* studies were performed at the same time of day to obviate circadian influences. The D2-Ahsg^{tm1Wja} mice (fetuin-KO mice) used in this study were derived from Ahsg-deficient C57BL/6-129/Sv hybrid mice by 10 backcrosses to pure DBA/2 genetic background mice obtained from a commercial breeder (17). Wild-type (WT) mice from this source were kept under identical conditions and served as control animals (Bomholdgard, Ry, Denmark).

BP Measurements

Mean BP was recorded in conscious 4- to 5-mo-old mice using a tail-cuff pressure transducer (BP-98A; Softron Co. Ltd., Tokyo, Japan). Values for each individual animal comprised 10 successive, averaged measurements obtained within approximately 5 min. Measurements were taken at the beginning of the active cycle, after the mice had become accustomed to a temperature-controlled restrainer within approximately 10 min.

Histology-Immunohistochemistry

For histology, tissues were dissected, fixed in formalin, and processed for paraffin or methylmethacrylate embedding. Sections were stained by von Kossa staining, hematoxylin and eosin, Safranin O, or picrosirius red as indicated. Methyl-Carnoy's fixative was used for immunohistochemical fibronectin staining. Sections were dewaxed and rehydrated. They then were boiled twice for 5 min in buffer (10 mM citric acid [pH 6.0]) and rinsed in tap water to retrieve antigens. Endogenous peroxidase was quenched with 0.03% H_2O_2 in methanol for 10 min, followed by a brief rinse in PBS and incubation in 4% horse serum (Vector Laboratories, Burlingame, CA) for 20 min. Polyclonal rabbit anti-rat (cross-reactive to mouse fibronectin) fibronectin antibody (Chemicon Inc., Temecula, CA) was added in blocking buffer (1% BSA in PBS) in a 1:50 dilution and incubated at 4°C for 1 h. After rinsing with PBS, biotinylated goat anti-rabbit antibody (Vector Laboratories) was added in blocking buffer in a dilution of 1:300 and incubated for 30 min at room temperature. Peroxidase ABC reagent and 3,3′-diaminobenzidine chromogenic substrate were applied following a commercial protocol (Vector Laboratories).

Cardiomyocyte Cell Number

For determining the number of myocytes in fetuin-KO and WT heart tissue, sections (thickness 4 μm) of paraffin-embedded myocardium were obtained and the nuclei were stained with the nucleic acid stain DAPI (4,6-diamidino-2-phenylindole). Seven mice per genotype were selected, and myocardial slices were examined by fluorescence microscopy at a magnification of 1:20. Two fields per section (0.2 mm^2 each) were randomly chosen and quantified (fetuin-KO tissue sections had to be free from fibrosis and calcification to be considered for quantification).

Calcium Measurement

Mice were anesthetized with isoflurane, and blood was drawn from the retro-orbital plexus. Freshly harvested tissue from the cardiac apex was snap-frozen in liquid nitrogen and stored at −80°C. Tissues were freeze-dried overnight. The median dry weight was 3.4 mg (range 1.5 to 8.5 mg) with a mean reduction factor wet/dry weight of 4.6 ± 0.6. Freeze-dried samples were extracted in 1 ml of 10% formic acid for 48 h. Calcium in the extracts was estimated at 422.7 nm wavelength using a Perkin Elmer PE4100 atomic absorption spectrometer (Boston, MA).

RNA Isolation and Absolute Quantitative Reverse Transcription Real-Time PCR

RNA was extracted following the RNAlater and RNeasy protocols (Qiagen, Hilden, Germany) with proteinase K digestion and on-column DNAse treatment. Reverse transcription and real-time PCR were performed on 200 ng of RNA using a commercial RT-PCR kit (Eurogentech, Cologne, Germany) and the ABI 7700 sequence detection system (PE; Applied Biosystems, Inc., Foster City, CA). The PCR reactions were performed in duplicate in 20-μl reaction mixtures that contained 2 μl of cDNA from the reverse transcription, 300 nM of each primer, and 100 nM of each probe (Eurogentech). TGF-β_1-specific primers were derived from EnsEmbl entry ENSMUST: 00000002678. Sense primer sequence was GCAACATGTGGAACTCTACCAGAA, antisense primer sequence was GACGTCAAAAGACAGCCACTCA, and probe sequence was FAM-ACCTTGGTAACCGGCTGCTGACCC-TAMRA, resulting in an amplicon length of 105 bp. Fibronectin-specific primers were derived from EnsEmbl entry ENSMUST: 00000055226. Sense primer sequence was GATGGAATCCGGGAGCTTTT, antisense primer sequence was TGCAAGGCAACCACACTGAC, and probe sequence was FAM-CCGGCCTGAGGCCCTGCA-TAMRA, resulting in an amplicon length of 107 bp. Collagen 4(1α)-specific primers were derived from EnsEmbl entry ENSMUST: 00000033898. Sense primer sequence was GGCGGTACACAGTCAGACCAT, antisense primer sequence was TGGTGTGCATCACGAAGGA, and probe sequence was FAM-CAGATTCCGCAGTGCCCTAACGGTT-TAMRA, resulting in an amplicon length of 89 bp. Annealing temperature was 60°C in all primer combinations. PCR amplicons were sized using agarose gel electrophoresis. An 18S ribosomal RNA probe (Applied Biosystems, Warnington, UK) was used as the internal standard for real-time PCR. Absolute mRNA quantification of samples was achieved by co-amplification of known quantities of pGEM-T plasmids (Promega, Madison, WI) that contained the cloned target genes (18S, TGF-β_1, fibronectin, and collagen 4[1α]) facilitating the calculation of target gene numbers per million copies of 18S RNA. Calculations were performed with the Sequence Detection Software (PE).

Langendorff Setup and Protocol

Preparation of murine hearts, explanted from age-matched (8 to 12 wk) fetuin-KO and WT mice (8 mice per group), was initiated. Retrograde perfusion at 100 mmHg constant pressure with modified Krebs-

Henseleit buffer was performed essentially as described, using a commercially available isolated heart apparatus (Hugo Sachs Elektronik, March-Hugstetten, Germany) (18). Perfusion pressure, perfusate oxygen concentration, aortic flow, left ventricular developed pressure (LVDP; the difference between minimal diastolic pressure and maximal systolic pressure), first derivative of left ventricular pressure over time (dP/dt), and heart rate were measured continuously. Hearts were stimulated at 600 beats per minute. After an equilibration phase of 30 min, baseline values were recorded. Thereafter, global no-flow ischemia was initiated and upheld for 16 min. Contractility parameters were recorded during 60 min of reperfusion. Heart wet weights were determined after termination of experiments.

The cardiac contractility index was calculated as dP/dt_{max} normalized for the respective LVDP. Likewise, the relaxation index (RI) was calculated as the ratio of dP/dt_{min} to respective LVDP.

Echocardiography

Conscious fetuin-KO and WT mice (six per group) that were matched for age (9 to 11 wk) and body weight (22 to 25 g) were examined by echocardiography on three separate occasions using a 15-MHz linear transducer connected to a Sonos 5500 (Philips Medical Systems, Hamburg, Germany) as described previously (19). At these times, mice received an intraperitoneal injection of isotonic saline solution (0.01 ml/g body wt, 0.9% NaCl, "placebo"), dobutamine (1.5 μg/g body wt; Solvay, Hannover, Germany), or atropine (0.1 μg/g body wt; Braun, Melsungen, Germany). Images were obtained within 7 and 11 min after intraperitoneal injection at the time of plateauing pharmacologic effects. For avoiding bradycardia, seen occasionally when performing echocardiography in conscious mice, animals were trained to tolerate the handling associated with echocardiographic examination on three to four separate occasions per day over a period of 3 d. When image recording of sufficient quality could not be initiated within 2 min, the animal was allowed to rest and images were obtained at a later time to ensure minimal time span of animal handling.

Statistical Analyses

Mean values with SD are reported. Groups were analyzed by ANOVA, followed by appropriate *post hoc* tests or *t* test if applicable. $P < 0.05$ was taken to indicate statistical significance (all statistical analysis calculated with SPSS 12.0; SPSS, Chicago, IL).

Results

Fibrous Remodeling in Calcified Myocardium of Fetuin-A$^{-/-}$ Mice

Necropsy of fetuin-KO mice revealed extensive, dystrophic calcification of myocardial tissue in both atrium and ventricle. Figure 1 illustrates typical views of adult 7-mo-old WT and fetuin-KO mice. In fetuin-KO mice, numerous spotted calcifications were visible even to the naked eye (Figure 1, A and B). Von Kossa staining demonstrated no calcification in WT mice (Figure 1, C and E). In contrast, extensive and widespread calcified lesions were stained throughout the myocardium of fetuin-KO mice (Figure 1, D, F, and G). The calcified lesions were surrounded by a dense fibrous capsule rich in collagen and fibronectin (Figure 1, H and I). Practically no cardiomyocytes were detected within calcified lesions, whereas the number of cardiomyocytes per volume remained unaltered in uncalcified segments of fetuin-KO hearts compared with WT hearts ($585 \pm 160 \times 10^3$ *versus* $589 \pm 142 \times 10^3$ cells/mm^3 fetuin-KO; $P = 0.78$). Importantly, the aorta of fetuin-KO mice did not show any calcification, fibrosis, or accumulation of fibronectin within the vessel wall. However, small peripheral vessels in skin and kidney were occasionally completely obliterated by calcium phosphate concrements (data not shown).

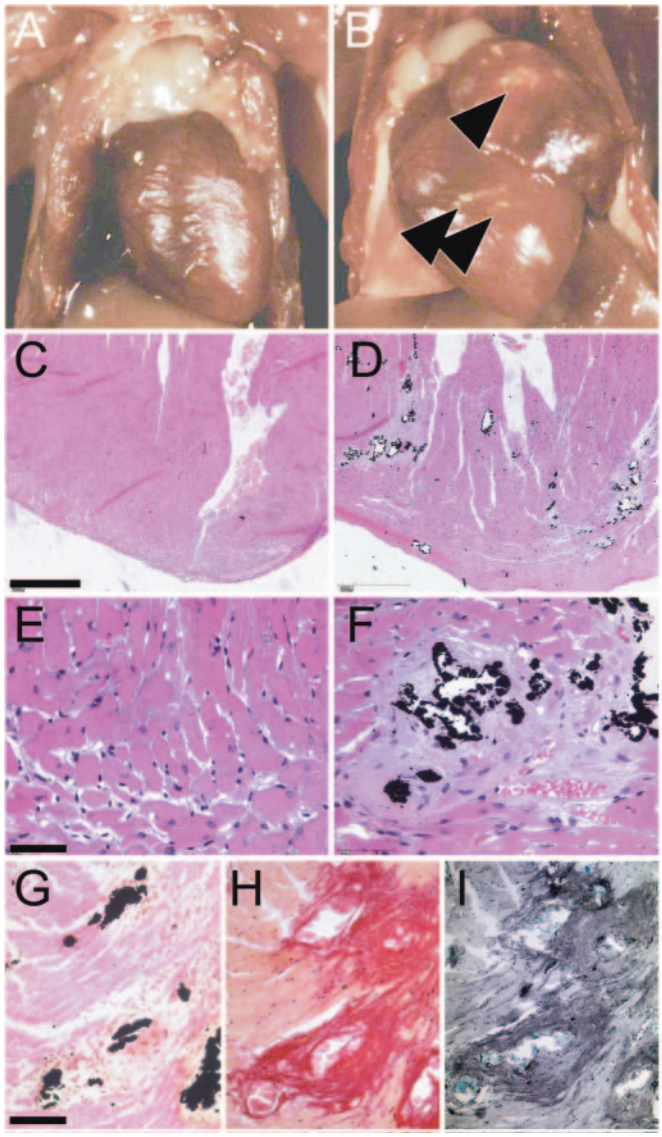

Figure 1. (A) Macroscopic view of hearts of wild-type (WT; A) and fetuin-A knockout (fetuin-KO; B) mice. Note off-white calcified lesions (arrowheads) in the heart of fetuin-KO mice. Low-power (C and D) and high-power (E and F) view of von Kossa–stained coronal sections of plastic-embedded myocardium of WT (C and E) and fetuin-KO (D and F) mice. Note the presence of von Kossa–positive calcified lesions in D and F surrounded by fibrous tissue. (G through I) Histochemical staining of paraffin-embedded myocardium shows that von Kossa–positive calcified deposits (G) are surrounded by a fibrous capsule rich in collagen (H) and fibronectin (I) as demonstrated by picrosirius red staining and immunohistochemistry, respectively. Bars = 500 μm in C, 50 μm in E, and 32 μm in G.

Calcium Content of Myocardium and mRNA Induction of Fibrosis-Associated Genes

Calcium content of myocardium was measured in 4.5- and in 7-mo-old WT and fetuin-KO mice using atomic absorption

spectroscopy. Figure 2A illustrates that fetuin-KO mice had up to 60-fold higher calcium content in myocardial tissue at both 4.5 and 7 mo of age (WT 4.5 mo: 0.014 ± 0.023, $n = 20$, and WT 7 mo: 0.016 ± 0.021, $n = 17$ *versus* fetuin-KO 4.5 mo: 0.811 ± 0.359, $n = 13$ [$P < 0.001$ *versus* WT]; and fetuin-KO 7 mo: 0.959 ± 0.418 μmol calcium/mg dry wt, $n = 13$ [$P < 0.001$]). On a dry weight basis, this corresponds to 4% total calcium content (40 μg/mg), suggesting that the myocardium of fetuin-KO animals had almost one tenth the calcium content of normal bone. Fetuin-A deficiency was associated with significant myocardial mRNA upregulation of the fibrogenic cytokine TGF-β1 (WT 170 ± 44.2 *versus* fetuin-KO 261 ± 62.0 copies of TGF-β1 per 1 million copies of 18S RNA; $n = 9$ per group; $P < 0.001$; Figure 2B). In line with this observation, collagen (1α) mRNA was upregulated 2.5-fold (WT 55 ± 23.6 *versus* fetuin-KO 124 ± 39.4 copies of collagen (1α) per 1 million copies of 18S RNA; $n = 9$ per group; $P < 0.001$), and fibronectin mRNA was induced eight-fold (WT 2 ± 1.0 *versus* fetuin-KO 16 ± 10.1 copies of fibronectin per 1 million copies of 18S RNA; $n = 9$ per group; $P < 0.001$). Similar alterations in mRNA levels of the above target genes were not found in the aortas of fetuin-KO mice. In summary, these data suggest TGF-β–stimulated matrix production in the myocardium but not in the aorta of fetuin-KO mice.

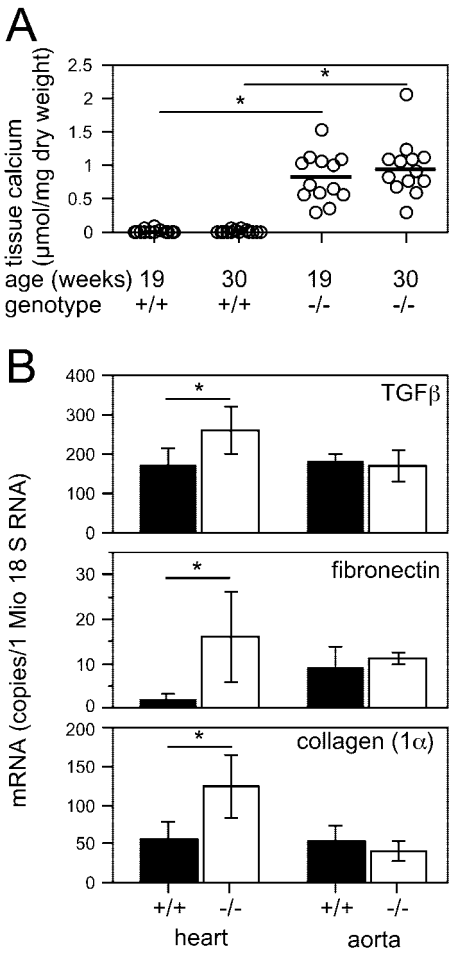

Figure 2. (A) Calcium content in myocardial tissues of WT (+/+) and fetuin-KO (−/−) mice. Tissues were harvested, freeze-dried, and extracted with acid, and the calcium content in the extract was estimated using atomic absorption spectroscopy. (B) mRNA induction of fibrosis-related gene products, TGF-β1, fibronectin, and collagen (1α) in WT and fetuin-KO mouse tissues. Messenger RNA amounts were estimated by TaqMan quantitative PCR as described in Materials and Methods and are given as number of copies per 1 million copies of 18S RNA ($n = 9$; *$P < 0.001$ using unpaired t test).

Contractile Function of Isolated, Saline-Perfused Hearts

Contractile function of hearts from fetuin-KO and WT mice was analyzed using the Langendorff perfused heart model. Heart wet weights did not differ between fetuin-KO and WT mice (fetuin-KO 173 ± 24 *versus* WT 178 ± 20 mg; $n = 8$ per group; NS). No difference was observed in coronary flow between fetuin-KO and WT mice (data not shown). Despite the significant myocardial calcification observed in fetuin-KO hearts (Figure 1), LVDP remained unimpaired (Table 1). Contractility as reflected by dP/dt_{max} (WT 4260 ± 682 *versus* fetuin-KO 4499 ± 472 mmHg/s; $n = 8$ per group; NS) or contractility index (CI = dP/dt_{max} normalized for LVDP; Table 1) likewise did not differ between the two groups. However, relaxation was significantly impaired in fetuin-KO hearts with the RI (RI = dP/dt_{min} normalized for LVDP) reduced by 23% compared with WT hearts ($n = 8$ per group; $P < 0.005$; Table 1), reflecting diastolic dysfunction. When subjected to 16 min of ischemia, initial recovery was similar in fetuin-KO and WT hearts (Figure 3). However, after this initial reperfusion phase (approximately 10 min), recovery in WT hearts proceeded to 91 ± 11% of preischemic LVDP within 60 min of reperfusion. In contrast, fetuin-KO hearts displayed a continuous decline in LVDP after the initial phase of reperfusion (Figure 3), resulting in 77 ± 15% of preischemic LVDP ($n = 8$ per group; $P < 0.05$ *versus* WT) after 60 min of reperfusion.

Hemodynamics of Conscious WT and Fetuin-KO Mice

The measurement of mean BP in conscious mice using a tail cuff revealed significant hypertension in fetuin-$A^{-/-}$ mice (systolic pressure: WT [$n = 13$] 113.6 ± 11.2 *versus* fetuin-KO [$n = 12$] 138.9 ± 10.8 mmHg; diastolic pressure: WT 68.2 ± 5.5 *versus* fetuin-KO 80.7 ± 8.7 mmHg; $P < 0.001$, respectively). Notably, we detected only a modest increase in pulse pressure

Table 1. Contractility and relaxation indices[a]

	WT	Fetuin-$A^{-/-}$
LVDP (mmHg)	105 ± 13	118 ± 16
CI (/s)	43 ± 1.8	45 ± 1.8
RI (/s)	−32 ± 2.1	−26 ± 1.9[b]

[a]Contractility index (CI) and relaxation index (RI; dP/dt_{max} and dP/dt_{min}, respectively, normalized for left ventricular developed pressure [LVDP]) of Langendorff perfused isolated hearts ($n = 8$ per group).

Fetuin-knockout mice showed significant impairment of RI ([b]$P < 0.005$) whereas other parameters of contractility remained at par with wild-type (WT) mice.

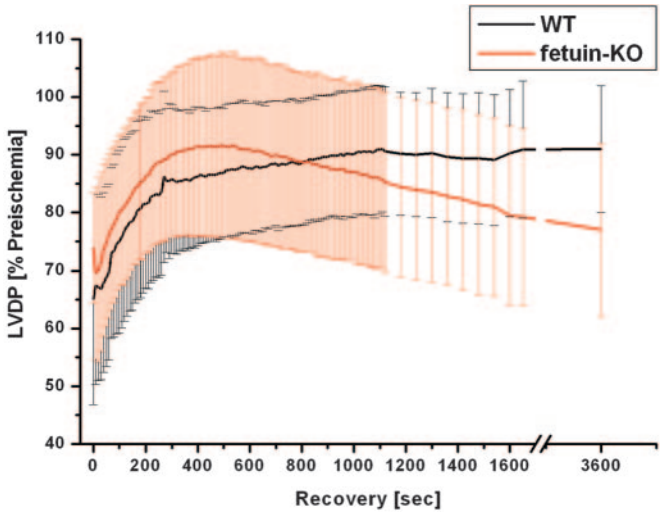

Figure 3. Ischemia-reperfusion. Fetuin-A$^{-/-}$ hearts showed poor recovery after 16 min of ischemia as compared with WT hearts. This was associated with 77 ± 15% of preischemic left ventricular developed pressure (LVDP) after 60 min of reperfusion compared with 91 ± 11% in WT mice ($n = 8$; $P < 0.05$).

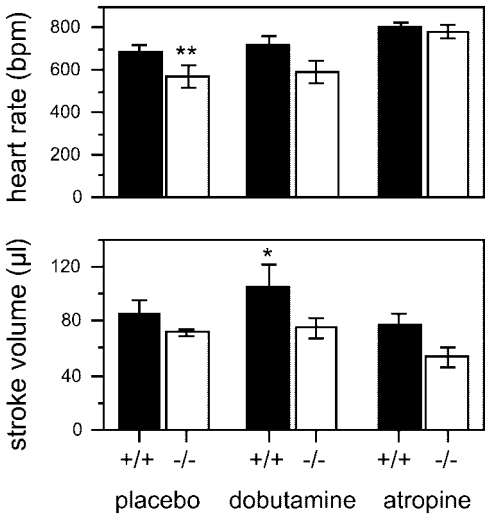

Figure 4. Stroke volume and heart rate in conscious mice. Heart rate was significantly depressed in fetuin-KO (−/−) compared with WT (+/+) mice (**$P < 0.001$; $n = 6$), whereas stroke volume was similar in both groups. Upon dobutamine stimulation, stroke volume increased by 17% in WT (*$P < 0.01$ *versus* placebo; $n = 6$), whereas fetuin-KO mice showed no increase in stroke volume (3%; $n = 6$; $P = 0.998$) or heart rate (4%; $n = 6$; $P = 0.88$ *versus* placebo). The decreased heart rate in fetuin-KO mice was reversed by treatment with atropine.

as a result of a concordant rise in diastolic pressure, indicating maintained aortic compliance.

Cardiac function was compared by echocardiography in conscious mice. Because of preconditioning (see Materials and Methods), animals remained calm during the entire examination. Two-dimensional and M-mode images as well as two-dimensional image-guided Doppler flow studies were obtained within an average of 3 ± 1 min. Figure 4 illustrates that heart rate was significantly depressed in fetuin-KO compared with WT mice, whereas stroke volume did not differ between the two groups. As a result, cardiac output of fetuin-KO mice was significantly reduced compared with WT mice (fetuin-KO 1.81 ± 0.18 *versus* WT 2.45 ± 0.29 ml/min per g; $n = 6$ per group; $P < 0.005$). The increased BP in fetuin-KO mice in conjunction with the impaired cardiac output suggests augmented vascular resistance in fetuin-KO mice.

After dobutamine stimulation (Figure 4), WT mice responded with a marked increase in cardiac output of 30% ($n = 6$; $P < 0.005$ *versus* placebo), composed of a 26% increase in stroke volume ($n = 6$; $P < 0.01$ *versus* placebo) and a 4% increase in heart rate ($n = 6$; NS *versus* placebo). In contrast, fetuin-KO mice showed only a marginal increase in stroke volume (3%; $n = 6$; NS *versus* placebo) and heart rate (4%; $n = 6$; NS *versus* placebo) with limited cardiac output augmentation (8%; $n = 6$; NS *versus* placebo and $P < 0.001$ *versus* WT+dobutamine) in comparison with WT mice (Figure 4).

For testing whether the observed lower heart rate of fetuin-KO mice might be due to a shift in sympathetic/parasympathetic tone, the parasympathetic tone was ablated by atropine treatment (0.1 µg/g). Seven minutes after atropine application, a similar heart rate of close to 800 beats per minute was measured by echocardiography in conscious fetuin-KO and WT animals. At this heart rate, decreased stroke volume was observed in both groups most probably related to decreased diastolic filling time. However, with increasing heart rate, stroke volume in fetuin-KO mice decreased significantly more (26%; $n = 6$; $P < 0.05$ *versus* placebo) than in WT mice (9%; $n = 6$; NS *versus* placebo), suggesting severe diastolic dysfunction in fetuin-KO mice.

Discussion

We report here on the structural and functional impact of severe myocardial calcification in fetuin-KO mice demonstrating cardiac fibrosis, diastolic dysfunction, impaired tolerance to ischemia, and catecholamine resistance in this model. This is the first study to evaluate the consequences of isolated myocardial calcification independent of any structural alterations of the vascular system. Our results may be clinically relevant especially for understanding the cardiovascular abnormalities and risks in the dialysis population, because both vascular and myocardial calcifications are highly prevalent in this patient group (11–15). This potential relevance is further supported by previous observations that patients on dialysis show decreased serum fetuin-A levels and that fetuin-A deficiency in uremia is associated with impaired cardiovascular survival (9).

Cardiac fibrosis in general and excessive collagen accumulation in particular are important factors in the pathogenesis of congestive heart failure in humans (20,21). Fibrotic left ventricular remodeling and stiffening in various forms of heart failure have recently been identified as therapeutic targets and essential components of diastolic dysfunction. In the hearts of fetuin-KO mice, we detected elevated mRNA expression of the fibrogenic cytokine TGF-β as well as two of its downstream target genes, collagen and fibronectin. In full accordance with

findings in human patients, the fibrosis in fetuin-KO hearts was associated with impaired relaxation, despite preserved LVDP and systolic contractility. It is interesting that in addition to its calcification inhibitory properties, fetuin-A can act as a TGF-β antagonist by acting as a soluble TGF-β receptor (4). In a state of fetuin-A deficiency, TGF-β loses one of its intrinsic antagonists and, mediated by binding to the AP-1 complex, may autoamplify its own expression, leading to enhanced fibrogenesis (22). We therefore conclude that the most plausible cause for the severe diastolic dysfunction observed in the fetuin-KO mice is extensive ventricular remodeling triggered by a combination of both cardiac calcification and fibrosis.

The lack of calcification of large- and middle-sized arteries in fetuin-KO mice is consistent with the finding that, unlike experimental rats, mice rarely ever calcify in their arteries with the notable exception of matrix Gla protein knockout mice (23). Accordingly, our studies showed that two arterial calcification inhibitors, matrix Gla protein and osteopontin, were upregulated on the RNA and protein level within the arterial wall of fetuin-A–deficient mice (W.R., K.M., J.-D.W., unpublished observations). The lack of overt arterial calcification in fetuin-KO mice greatly facilitates the interpretation of our findings concerning cardiac hemodynamics. This phenotype excludes an indirect confounding influence of arterial stiffness on cardiac function and remodeling, which is thought to be critically involved in the development of calcification-associated heart failure, *e.g.*, in uremic patients (24). The significant alterations in cardiac function found in this model suggest that myocardial calcification *per se* may be a hitherto underestimated factor in the pathogenesis of congestive heart failure.

Amann *et al.* (25) observed that rats that underwent subtotal nephrectomy and were fed a high-phosphorus diet developed cardiac fibrosis and intramyocardial arterial remodeling. Subsequently, these authors (26) showed that reduced renal function in this model was associated with a significantly increased cardiomyocyte volume and reduced number of cardiomyocytes as well as postcoronary microvascular damage. In contrast, the number (and thus the volume) of cardiomyocytes in our model remains unaltered in areas not affected by calcification, whereas practically no cardiomyocytes are found in tissue sections with calcification. As heart weight is not increased in fetuin-KO, the absolute number of cardiomyocytes per heart must be decreased in fetuin-KO as a result of significant loss of contractile tissue to calcification linked remodeling. Thus, preservation of cardiac function at rest in fetuin-KO mice is likely due to critical compensatory activation of the remaining cardiomyocytes' contractile reserve, a notion that is further supported by the significantly impaired response of fetuin-KO mice to β1 stimulation. Although speculative, it is a possible concept that the compensatory inotropic activation in fetuin-KO is mediated through increased intracellular calcium levels, albeit high intracellular calcium levels are also associated with negative lusitropic effects, with the latter being clearly visible in our model. Cardiac changes observed in patients with ESRD reflect alterations observed in both animal models, namely structural cardiomyocyte alterations and microvascular damage as seen in rats with 5/6 subtotal nephrectomy, interstitial fibrosis as seen in both models, and severe interstitial calcification with impaired diastolic function as observed in fetuin-KO mice.

An important compensatory mechanism in fetuin-KO mice was revealed when heart rate was measured during echocardiography. This decreased heart rate compared with that of WT mice may contribute to a reduction of cardiac energy demand. This might be important in fetuin-KO mice because increased left ventricular stiffness, in conjunction with increased afterload as a result of high BP levels, would contribute to an overtly high left ventricular wall strain and thus high energy demand. In addition, lower heart rates primarily extend diastole duration and thus optimize filling of these stiff ventricles. The observed heart rate decrease of fetuin-KO mice was achieved by a shift in sympathetic/parasympathetic tone toward the latter, as demonstrated by our atropine experiments. Ablation of this increased parasympathetic tone provoked a pronounced decline in stroke volume in fetuin-KO mice, prohibiting normalization of cardiac output despite significantly increased heart rate, thereby again underscoring the functional relevance of diastolic dysfunction in fetuin-KO mice.

The dampened response to β1 stimulation that was documented in fetuin-KO mice could also be interpreted as a mechanism that protects the heart from critical increases in energy demand and thus as a further compensating mechanism. Nevertheless, the decreased β1 sensitivity and the impaired cardiac output observed in fetuin-KO mice are indicators of the failing heart. In this context, an impaired sympathetic response is observed in severely ill dialysis patients, contributing to hemodynamic instability during hemodialysis sessions (27). At least in this patient group, this impaired response might be indicative of structural myocardial damage rather than active compensation.

The highly pathologic response to ischemia-reperfusion injury further supports our interpretation that fetuin-KO hearts may serve as a suitable model for the human failing heart. Ultimately, the severe deterioration of ventricular function after brief initial recovery in fetuin-KO hearts suggests myocardial damage possibly as a result of impaired oxygenation during reperfusion secondary to high ventricular wall stress. This pathomechanism could potentially contribute to recent clinical observations demonstrating poor outcome in patients with chronic kidney disease after acute myocardial infarction (28,29).

Although no null fetuin-A mutations have yet been described in humans, decreased fetuin-A levels in humans have been linked to vascular calcification and increased mortality as observed in patients on dialysis (9,30–32). These patients have a several-fold increased cardiovascular mortality risk, which is associated with the severity of cardiovascular calcification, but do not exclusively or typically die of major coronary events such as those caused by plaque rupture (12,13). The causes of cardiovascular death in dialysis patients span the wide range of myocardial infarction, sudden death, arrhythmia, congestive heart failure, stroke, and maybe additional less well-defined events. Given our results, myocardial calcification and resulting myocardial stiffness may be one additional independent and as yet underestimated factor contributing to the cumulative cardiovascular risk in uremia. Myocardial dysfunction thus may

be caused not only indirectly by ischemic heart disease, left ventricular hypertrophy, arterial stiffness, and anemia, respectively, but also directly by intramyocardial calcification. With cardiovascular disease increasingly viewed as partly mediated by inflammatory processes, the negative acute-phase protein fetuin-A might prove a prime candidate and a valuable therapeutic target in preventing dystrophic cardiovascular calcification and fibrosis and thus unwanted aspects of left ventricular remodeling, especially in a high-risk population such as dialysis patients.

Acknowledgments

This work was supported in part by Deutsche Forschungs Gemeinschaft Grant ME 1821 to M.W.M. and JA 562 to W.J.D. as well as IZKF BIOMAT to M.W.M. and W.J.D.

We thank S. Becher and I. Moshkova for excellent technical assistance.

References

1. Dziegielewska KM, Brown WM: *Fetuin*, Heidelberg, Springer-Verlag, 1995
2. Triffitt JT, Gebauer U, Ashton BA, Owen ME, Reynolds JJ: Origin of plasma alpha2HS-glycoprotein and its accumulation in bone. *Nature* 262: 226–227, 1976
3. Keeley KW, Sitarz EE: Identification and quantitation of alpha 2-HS-glycoprotein in the mineralized matrix of calcified plaques of atherosclerotic human aorta. *Atherosclerosis* 55: 63–69, 1985
4. Demetriou M, Binkert C, Sukhu B, Tenenbaum HC, Dennis JW: Fetuin/alpha2-HS glycoprotein is a transforming growth factor-beta type II receptor mimic and cytokine antagonist. *J Biol Chem* 271: 12755–12761, 1996
5. Heiss A, DuChesne A, Denecke B, Grotzinger J, Yamamoto K, Renne T, Jahnen-Dechent W: Structural basis of calcification inhibition by alpha 2-HS glycoprotein/fetuin-A. Formation of colloidal calciprotein particles. *J Biol Chem* 278: 13333–13341, 2003
6. Price PA, Lim JE: The inhibition of calcium phosphate precipitation by fetuin is accompanied by the formation of a fetuin-mineral complex. *J Biol Chem* 278: 22144–22152, 2003
7. Reynolds JL, Joannides AJ, Skepper JN, McNair R, Schurgers LJ, Proudfoot D, Jahnen-Dechent W, Weissberg PL, Shanahan CM: Human vascular smooth muscle cells undergo vesicle-mediated calcification in response to changes in extracellular calcium and phosphate concentrations: A potential mechanism for accelerated vascular calcification in ESRD. *J Am Soc Nephrol* 15: 2857–2867, 2004
8. Schafer C, Heiss A, Schwarz A, Westenfeld R, Ketteler M, Floege J, Muller-Esterl W, Schinke T, Jahnen-Dechent W: The serum protein alpha2-Heremans-Schmid glycoprotein/fetuin-A is a systemically acting inhibitor of ectopic calcification. *J Clin Invest* 112: 357–366, 2003
9. Ketteler M, Bongartz P, Westenfeld R, Wildberger JE, Mahnken AH, Bohm R, Metzger T, Wanner C, Jahnen-Dechent W, Floege J: Association of low fetuin-A (AHSG) concentrations in serum with cardiovascular mortality in patients on dialysis: A cross-sectional study. *Lancet* 361: 827–833, 2003
10. Giachelli CM: Ectopic calcification: Gathering hard facts about soft tissue mineralization. *Am J Pathol* 154: 671–675, 1999
11. Schwarz U, Buzello M, Ritz E, Stein G, Raabe G, Wiest G, Mall G, Amann K: Morphology of coronary atherosclerotic lesions in patients with end-stage renal failure. *Nephrol Dial Transplant* 15: 218–223, 2000
12. London GM, Guerin AP, Marchais SJ, Metivier F, Pannier B, Adda H: Arterial media calcification in end-stage renal disease: Impact on all-cause and cardiovascular mortality. *Nephrol Dial Transplant* 18: 1731–1740, 2003
13. Wang AY, Wang M, Woo J, Lam CW, Li PK, Lui SF, Sanderson JE: Cardiac valve calcification as an important predictor for all-cause mortality and cardiovascular mortality in long-term peritoneal dialysis patients: A prospective study. *J Am Soc Nephrol* 14: 159–168, 2003
14. Eguchi M, Tsuchihashi K, Takizawa H, Nakahara N, Hagiwara M, Ohnishi H, Torii T, Hashimoto A, Marusaki S, Nakata T, Ura N, Shimamoto K: Detection of cardiac calcinosis in hemodialysis patients by whole-body scintigraphy with 99m-technetium methylene diphosphonate. *Am J Nephrol* 20: 278–282, 2000
15. Rostand SG, Sanders C, Kirk KA, Rutsky EA, Fraser RG: Myocardial calcification and cardiac dysfunction in chronic renal failure. *Am J Med* 85: 651–657, 1988
16. Guerin AP, London GM, Marchais SJ, Metivier F: Arterial stiffening and vascular calcifications in end-stage renal disease. *Nephrol Dial Transplant* 15: 1014–1021, 2000
17. Jahnen-Dechent W, Schinke T, Trindl A, Muller-Esterl W, Sablitzky F, Kaiser S, Blessing M: Cloning and targeted deletion of the mouse fetuin gene. *J Biol Chem* 272: 31496–31503, 1997
18. Merx MW, Flogel U, Stumpe T, Godecke A, Decking UK, Schrader J: Myoglobin facilitates oxygen diffusion. *FASEB J* 15: 1077–1079, 2001
19. Merx MW, Liehn EA, Janssens U, Lutticken R, Schrader J, Hanrath P, Weber C: HMG-CoA reductase inhibitor simvastatin profoundly improves survival in a murine model of sepsis. *Circulation* 109: 2560–2565, 2004
20. Heeneman S, Cleutjens JP, Faber BC, Creemers EE, van Suylen RJ, Lutgens E, Cleutjens KB, Daemen MJ: The dynamic extracellular matrix: Intervention strategies during heart failure and atherosclerosis. *J Pathol* 200: 516–525, 2003
21. Kass DA, Bronzwaer JG, Paulus WJ: What mechanisms underlie diastolic dysfunction in heart failure? *Circ Res* 94: 1533–1542, 2004
22. Kim SJ, Angel P, Lafyatis R, Hattori K, Kim KY, Sporn MB, Karin M, Roberts AB: Autoinduction of transforming growth factor beta 1 is mediated by the AP-1 complex. *Mol Cell Biol* 10: 1492–1497, 1990
23. Luo G, Ducy P, McKee MD, Pinero GJ, Loyer E, Behringer RR, Karsenty G: Spontaneous calcification of arteries and cartilage in mice lacking matrix GLA protein. *Nature* 386: 78–81, 1997
24. Blacher J, Guerin AP, Pannier B, Marchais SJ, London GM: Arterial calcifications, arterial stiffness, and cardiovascular risk in end-stage renal disease. *Hypertension* 38: 938–942, 2001
25. Amann K, Tornig J, Kugel B, Gross M-L, Tyralla K, El-Shakmak A, Szabo A, Ritz E: Hyperphosphatemia aggravates cardiac fibrosis and microvascular disease in experimental uremia. *Kidney Int* 63: 1296–1301, 2003
26. Amann K, Tyralla K, Gross M-L, Schwarz U, Törnig J, Haas

CS, Ritz E, Mall G: Cardiomyocyte loss in experimental renal failure: Prevention by ramipril. *Kidney Int* 63: 1708–1713, 2003
27. Pelosi G, Emdin M, Carpeggiani C, Morales MA, Piacenti M, Dattolo P, Cerrai T, Macerata A, L'abbate A, Maggiore Q: Impaired sympathetic response before intradialytic hypotension: A study based on spectral analysis of heart rate and pressure variability. *Clin Sci (Lond)* 96: 23–31, 1999
28. Langston RD, Presley R, Flanders WD, McClellan WM: Renal insufficiency and anemia are independent risk factors for death among patients with acute myocardial infarction. *Kidney Int* 64: 1398–1405, 2003
29. Wright RS, Reeder GS, Herzog CA, Albright RC, Williams BA, Dvorak DL, Miller WL, Murphy JG, Kopecky SL, Jaffe AS: Acute myocardial infarction and renal dysfunction: A high-risk combination. *Ann Intern Med* 137: 563–570, 2002
30. Stenvinkel P, Wang K, Axelsson J, Axelsson J, Pecoits-Filho R, Gao P, Barany P, Lindholm B, Jogestrand T, Heimburger O, Holmes C, Schalling M, Nordfors L: Low fetuin-A levels are associated with cardiovascular death: Impact of variations in the gene encoding fetuin. *Kidney Int* 67: 2383–2392, 2005
31. Ketteler M, Wanner C, Metzger T, Bongartz P, Westenfeld R, Gladziwa U, Schurgers LJ, Vermeer C, Jahnen-Dechent W, Floege J: Deficiencies of calcium-regulatory proteins in dialysis patients: A novel concept of cardiovascular calcification in uremia. *Kidney Int Suppl* 63: S84–S87, 2003
32. US Renal Data System: USRDS 1999 annual data report. *Am J Kidney Dis* 34: S87–S94, 1999